Inhomogeneities in plastically deformed silicon single crystals. I. ESR and photo-ESR investigations of *p*- and *n*-doped silicon

C. Kisielowski, J. Palm, B. Bollig, and H. Alexander
Abteilung für Metallphysik, II. Physikalisches Institut, Universität zu Köln, Zülpicherstrasse 77, D-5000 Köln 41, Germany
(Received 21 August 1990)

A quantitative analysis is given for three distinguishable effects contributing to inhomogeneities of the band gap of plastically deformed and doped silicon: (a) capture of charge from the chemical dopants to deep-point-like defects, (b) capture of the charge by deep defects in the core of dislocations, and (c) capture of the charge into states split off from the band edges that are caused by the presence of dislocations in the crystals. In crystals deformed below 700 °C process (a) dominates and it gives rise to local shifts of the band edges. Contributions from processes (a) and (b) can be distinguished by only analyzing the ESR spectra of the deformed samples, but they do not lead to an accumulation of delocalized charge along the dislocations, which, in the case of process (c), is shown to be evident from the appearance of electric-dipole spin resonances. Observation of the last process requires special deformation procedures that produce straight dislocation segments.

I. INTRODUCTION

There is a considerable amount of work done in the field of doping effects on the defect spectrum of deformed silicon. It is reviewed in Refs. 1 and 2. One of the major goals of these studies is devoted to the question of how large the charge captured by dislocations could be? However, its determination is related with uncertainties because it is necesary to know which of the deformation-induced defects should be attributed to dislocations. It is a well-known fact that apart from dislocations and related defects plastic deformation introduces a large concentration of ordinary point defects into the crystals which can be separated by means of special detection techniques.[3] Electron-spin resonance (ESR) is one of the few suitable tools to distinguish between both types of defects. Trying to understand the electrical properties of deformed crystals a quantitative analysis of the contribution from both types of defects is necessary. This requires us to link the structural information obtainable from ESR spectroscopy to electrical measurements such as deep-level transient spectroscopy (DLTS) and it is possible using photo-ESR because, thereby, a particular ESR signal can be related to a certain energy level in the band gap.

In phosphorous-doped silicon the concentration of electrons trapped in deep states can be determined by the decrease of the P^0 ESR signal as long as the energy levels are deeper than the shallow P^0 donors ($E_c - 0.045$ eV), because the reaction $P^0 \rightarrow P^+ + e$ takes place. Since there is agreement that plastic deformation of *n*-type silicon leads to the formation of deep acceptorlike states,[2] the investigation of the P^0 ESR signal will be used extensively. The ESR signal of the shallow acceptors in *p*-type material is rather sensitive to deformation-induced strain fields, which is why such an analysis is not possible in this case.[4]

The paper is divided into two parts. In the first part ESR and photo-ESR results are presented. The second part deals with DLTS measurements. In particular we tried to investigate comparably deformed or identical samples by ESR and DLTS, which required special ESR detection modes (Sec. II) and certain doping levels because very often both methods exclude each other: DLTS requires doped samples but conducting samples destroy the quality factors of the cavities used for the ESR measurements.

It is the goal of this paper to show quantitatively that three distinguishable types of defects compensate shallow dopants. In crystals deformed below 700 °C the dominant compensating defects are point defects (type I). Their concentration clearly exceeds the concentration of the defects in the core of dislocations (type II; Secs. III A and III B). A dependence of the P^0-ionization on the initial doping level is used to show that the deep-defect distribution is inhomogeneous with respect to the distribution of the dopants (Sec. III C). Photo-ESR confirms the results and provides a tool for the separation of deep from shallow deformation-induced defects (type III; Sec. III D). This distinction finds additional support by use of special deformation procedures (Sec. III E). A quantitative determination of defect concentrations is possible if the inhomogeneous defect distribution is taken into account (Sec. III F).

II. EXPERIMENTAL PROCEDURES

Samples of the size $4 \times 4 \times 16$ mm^3 were plastically compressed along their long [213] axes at $T_d = 650$ °C, which favors a single slip in the main slip system[011], (1$\underline{1}$1). Only the central homogeneously deformed parts of the crystals were used for the experiments. Table I lists the material properties and the deformation parameters of the samples.

In the progress of the investigations it turned out that

TABLE I. List of deformed samples. Floating-zone silicon doped with boron or phosphorus. Initial dislocation density $\approx 10^4$ cm^{-2} in all cases. Deformation temperature $T_d = 650$ °C.

Sample	Doping (cm^{-3})	$\epsilon = \delta l/l$ (%)	τ (MPa)	Gas amb.
a	$p = 3\times10^{12}$	2.8	30	N_2 (92%), H_2 (8%)
b	$p = 5\times10^{14}$	5.0	30	N_2 (92%), H_2 (8%)
c	$p = 4\times10^{15}$	7.5	40	N_2 (92%), H_2 (8%)
d	$p = 4\times10^{15}$	2.8	30	N_2 (92%), H_2 (8%)
e	$p = 3.2\times10^{16}$	2.7	30	N_2 (92%), H_2 (8%)
f	$p = 4.8\times10^{17}$	3.0	30	Ar
g	$n = 4.4\times10^{15}$	5.7	60	N_2 (92%),H_2 (8%)
h	$n = 4.4\times10^{15}$	3.8	30	N_2 (92%),H_2 (8%)
i	$n = 4.4\times10^{15}$	2.8	30	N_2 (92%), H_2 (8%)
j	$n = 5\times10^{16}$	5.7	30	Ar
k	$n = 4\times10^{17}$	2.8	30	Ar

the presence of hydrogen in the forming gas atmosphere (92% N_2, 8%, H_2) during the deformations may affect the defect spectrum. This is why part of the samples were deformed in argon atmosphere later on. However, it has been shown that a special deformation procedure is required to introduce molecular hydrogen into the crystals[5] which was not used here. Nevertheless, the gas ambient is listed also in Table I. Annealing experiments at 800 °C were done in a forming gas atmosphere and the results turned out to be not different from those of control samples annealed in argon.

The ESR measurements were performed with a modified Bruker BER 420 *X*-band spectrometer which allows for lock-in detection of dispersion and absorption signals with variable magnetic-field modulaton frequencies ν_m (100 Hz $\leq \nu_m \leq$ 100 kHz). In deformed intrinsic silicon the two signals, namely, the high-temperature (HT) and the low-temperature (LT) signal, are related to point defect clusters (including Si *K*3, *K*4, *K*5, and pentavacancies) and to dislocation related defects (Si *Y* and Si *K*1), respectively.[3] Since both types of signals have different spin-lattice relaxation times T_1 [with T_1 (HT signal) $\gg T_1$ (LT signal)] the HT signal can be detected by ESR absorption measurements at temperatures $T_m \geq 80$ K, only.[6] Since doped samples are conducting at such temperatures the skin depth δ must be large compared with the sample thickness to obtain ESR signals. At doping levels of $\approx 10^{15}$ cm^{-3} ($\delta \approx 1$ mm) this could be realized with samples of ≈ 100 μm thickness in the *X*-band spectrometer. However, the recorded signals might be smaller in such samples because the microwave fields will be attenuated with increasing sample thickness and signal accumulation was used to increase the signal-to-noise ratio. For higher doping levels the signal detection needs to be done in the freeze-out range of the free-carrier concentration. From the analysis of the deformation-induced defects in intrinsic silicon[6] together with some experimental tests it turned out that HT signals in doped samples can be measured best by detection of their dispersion signals (χ_0') in phase with the magnetic-field modulation at 24 K and the LT signals by either measuring the absorption at ≈ 15 K or their dispersion out-of-phase signals (χ_{90}') at 8 K; the latter detection mode having the additional advantage of suppressing signals with other spin-lattice relaxation times such as the P^0 resonance which otherwise was subtracted from the spectrum by help of a computer. Details of the installation for optical excitation can be found in Ref. 7.

III. RESULTS

A. Weakly doped samples ($[n], [p] \leq 5\times10^{15}$ cm^{-3})

The 300-K ESR absorption spectrum of the intrinsic sample (*a*) is shown in Fig. 1, curve (*a*). Comparison with Fig. 1, curve (*c*) demonstrates that *n* doping reduces the signal of the otherwise equally deformed sample. It is possible to generate different stages of the spectrum between the two curves [(*a*) and (*c*)] by controlling the amount of strain which determines the number of deep defects introduced by the deformation.[6] Curve (*b*) shows such an intermediate stage. Comparison of the three spectra in Fig. 1 also suggests that there is only one new signal marked by *e*. From its *g* value and its isotropy it is attributed to the resonance of free electrons in the conduction band. The weakly structured signal of the doped samples contributes to the background of the ESR spectrum in the undoped sample which could be revealed by successive destruction of parts of the signal by hydrogen.[5,8]

Thus, the signal intensity is controlled by the effective doping $n_e = (N_{cd} - N_a)$ (N_{cd} = concentration of chemical donors, N_a = concentration of deformation-induced acceptors; we assume $N_a \gg N_d$ with N_d = concentration of deformation-induced donors because of the amphotericity of the deformation-induced defects to trap electrons in *n*-type material and holes in *p*-type material as shown later on): the larger n_e the more defects vanish from the 300-K signal. This indicates that the position of the Fermi level E_f determines the paramagnetism of these defects. Figure 2 shows the temperature dependence of the absorption spectrum of sample *h*. It can be seen that its shape changes only a little in the temperature range 300 K $\geq T_m \geq$ 80 K. This is in contrast to what is known from the intrinsic samples, where around $T_m \approx 220$ K a sharp change of the signal shape is always observable.[3] Thus, E_F controls this effect, too. The transition from

the HT spectrum to the LT spectrum between 80 $K \geq T_m \geq 10$ K remains the same just as in case of intrinsic silicon because it is caused by saturation effects.[3,6]

In addition it can be seen in Fig. 2 that the free electrons detectable at 180 K freeze out on the phosphorus atoms giving rise to the signal of isolated and neutral phosphorus at 15 K the hyperfine splitting of which is caused by its nuclear spin ($I = \frac{1}{2}$). The presence of this signal proves that at least in part of the crystal E_F is close to the level of the shallow donor.

A similar situation is detected in p-type samples: low doping of strongly deformed samples leads to a similar spectrum as that of the intrinsic material [Fig. 3, curve (a), Fig. 1, curve (a)]. The sharp lines of the 300-K spectra increase with the effective p doping $p_e = (N_{ca} - N_d)$ (N_{ca} denotes concentration of chemical acceptors; we assumed in p-type material $N_d \gg N_a$ because of the amphoteric property of the deformation-induced defects) and in the central part of the spectra no additional lines appear [Fig. 3, curves (b) and (c)]. However, at their wings a series of additional (peripheral) anisotropic lines are present that are rather similar to what has been reported in Ref. 9. But they were not analyzed in this work. The temperature dependence of the spectrum of sample (c) (Fig. 4), in particular, also shows no change of the signal

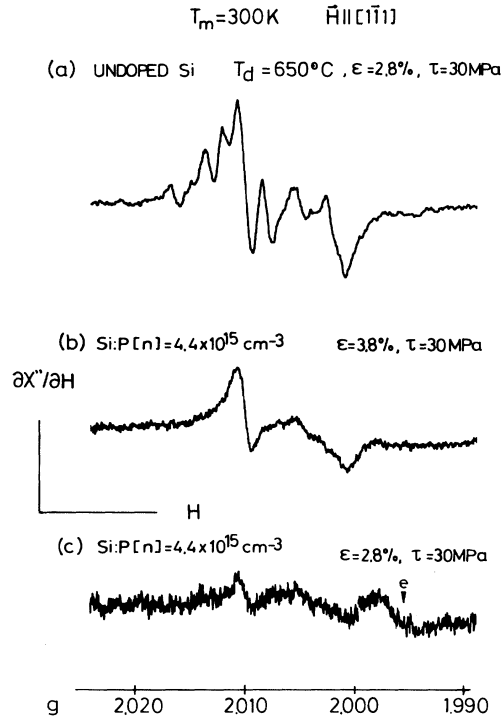

FIG. 1. ESR absorption spectrum of the intrinsic sample a [(a)] and two n-type samples h [(b)] and i [(c)] (samples labeled in Table I) measured at 300 K. Deformation parameters and the initial doping concentration [n] are indicated. "e" marks the resonance of electrons in the conduction band. The plotted spectra are linearly scaled to a strain of $\epsilon = 2.7\%$ for the purpose of comparison.

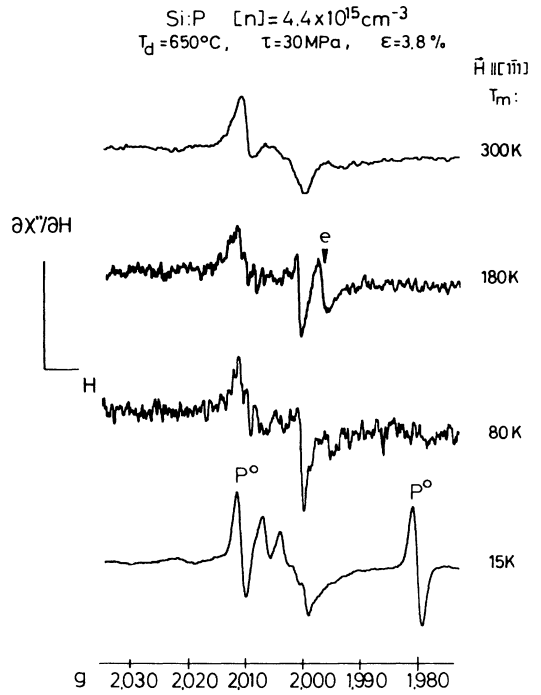

FIG. 2. Temperature dependence of the ESR absorption spectrum of sample h. P^0 indicates the resonance of isolated and neutral P atoms which are paramagnetic because electrons from the conduction band (e) are frozen out on the donor atoms at 15 K. The different noise of the spectra results from different accumulations.

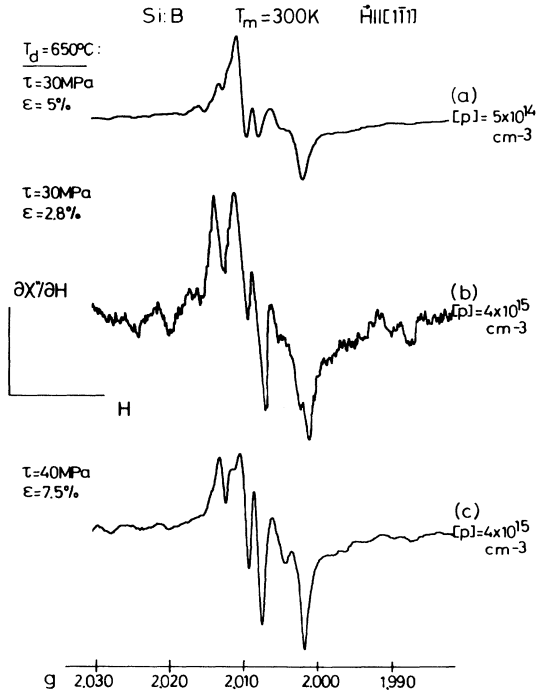

FIG. 3. ESR absorption spectra of the p-type samples b [a], d [(b)], and c [(c)] measured at 300 K. Deformation parameters and the initial doping concentration [p] are indicated. The plotted spectra are linearly scaled to a strain of 2.7% and comparable with Fig. 1.

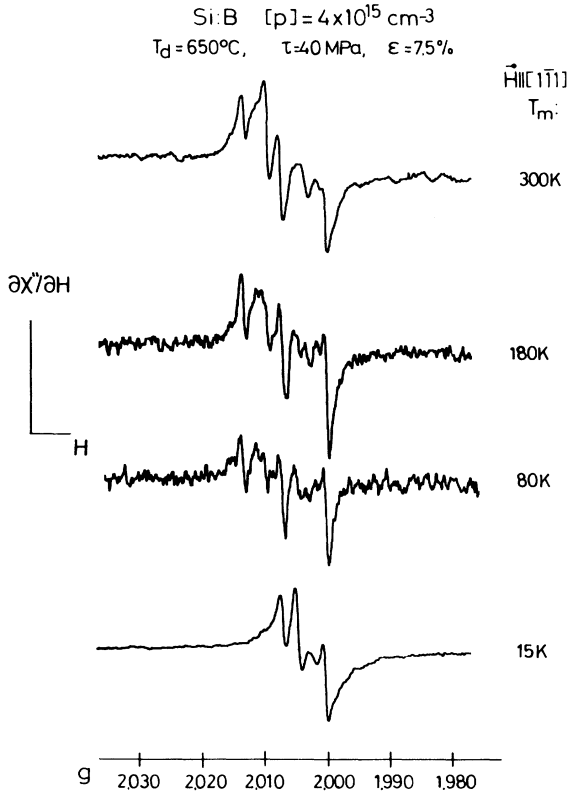

FIG. 4. Temperature dependence of the ESR absorption spectrum of sample *c*. At 15 K the three sharp lines of the Si $K1$ center can be seen on the background signal called Si Y. In Fig. 2 they are superimposed by the P^0 resonance and smaller in comparison with Si Y.

shape around $T_m \approx 220$ °C and at 15 K Si $K1$ and Si Y can be recorded. From these measurements it can be concluded as follows.

The change of the defect spectrum in intrinsic silicon observable at ≈ 220 K depends on the position of the Fermi level.

In the range of weak doping $\approx 10^{15}$ cm^{-3} the 300-K ESR absorption signal is influenced by E_F; the largest signal is observed in p-type material while n doping leads to a signal reduction.

B. Heavily doped samples ($[p], [n] \geq 5\ 10^{15}$ cm^{-3})

In heavily doped samples the HT and the LT signal was measured by detection of the dispersion signals for reasons mentioned in Sec. II. Two typical spectra and the dependence of the integrated signals ($A = \int \chi' dH$) on the doping are shown in Fig. 5. In order to check whether photo-ESR is possible or not the samples were illuminated with white light at the detection temperature. It can be seen that n doping reduces the HT signal up to $\approx 75\%$, there is a maximum in the weak p doping range and the signal decreases for higher p doping. The HT signals detected in materials with doping levels $p \approx n \approx 5 \times 10^{17}$ cm^{-3} are not included in the figure: In the p-type material we observed Si $K5$ lines at 8 K which is only possible if the spin-lattice relaxation time of this point defect center (part of the HT signal) is strongly reduced by doping. In this case its intensity cannot be compared with the one of the other samples because it depends on T_1. In the n-type sample it was just no longer possible to separate the HT signal from the strong P^0 resonance. With increasing n doping the HT signal can be

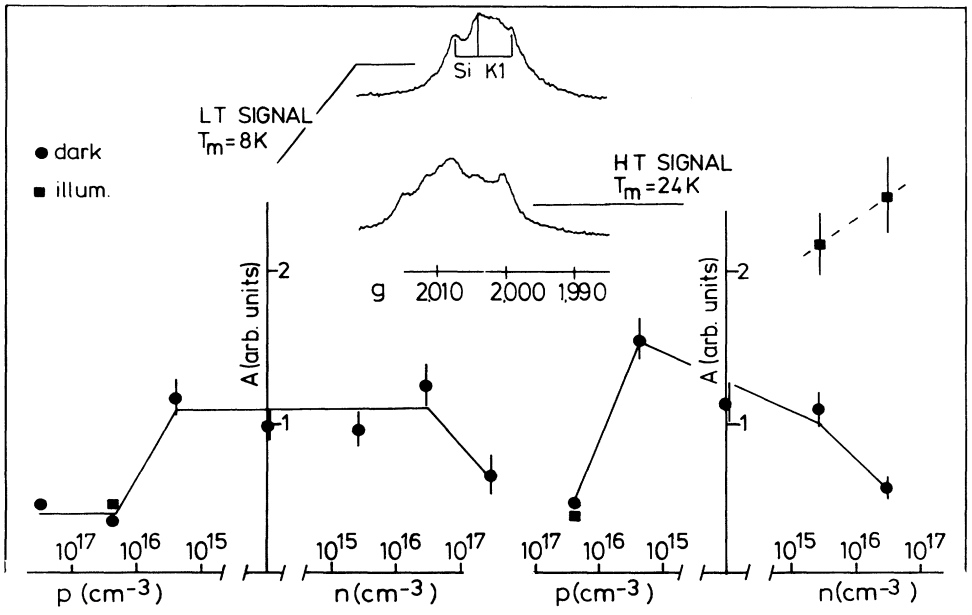

FIG. 5. Integrated intensity $A = \int \chi' dH$ of the LT and the HT signals of samples *a*, *d*, *e*, *f*, *i*, *j*, and *k*. The inset shows the spectra of sample *e*. Detection temperatures are indicated. The HT signal was measured in phase with respect to the magnetic-field modulation frequency and the LT one with a phase shift of 90° (Ref. 6). Using the linear dependence of the signal intensities on plastic strain (Ref. 6) the signals of all samples were scaled to a strain of $\epsilon = 2.7\%$ which is important for sample *j*, only.

TABLE II. Concentration of ionized P atoms in deformed samples ($T_d = 650$ °C; $\tau = 30$ MPa) with different initial doping concentrations n. The influence of the gas ambient and of a predeformation ($T_d = 800$ °C; $\tau = 8$ MPa; $\epsilon = 1.6\%$) with a following annealing procedure ($t_a = 16$ h) are also investigated. The experimental error for the absolute values is $\approx 10\%$.

	Initial doping (cm^{-3})	Predeform.	Main deform. ϵ (%)	Gas ambient	$[P^+]$ (cm^{-3})
1:	4.4×10^{15}	no	2.8	N_2 (92%),H_2 (8%)	3.1×10^{15}
2:	4.4×10^{15}	yes	2.8	H_2	3.8×10^{15}
3:	1.1×10^{16}	no	2.7	Ar	7.3×10^{15}
4:	1.1×10^{16}	yes	2.7	H_2	7.8×10^{15}
5:	1.1×10^{16}	yes	3.7	Ar	9.1×10^{15}
6:	1.1×10^{16}	yes	3.7	H_2	8.4×10^{15}

enhanced by photoexcitation while in the p region such an excitation leads to a weak decrease of the signal.

In contrast the LT signal intensity does not depend on weak doping and drops for both, high-p or high-n doping. It has bee shown that Si $K1$ is affectable by doping.[7] However, it is clear from the inset of Fig. 5 that Si $K1$ is only a small contribution to the LT signal (5–10%) which lies within the experimental error of the integration procedure used to determine A. Thus, the plot shows the doping dependence of Si Y, only. A 30% increase of Si Y is observed in the strong p-doping range by white-light excitation.

C. Ionization of the P^0 donor

By investigating n-type material, it is possible to determine the concentration of electrons trapped to deep-level defects by comparing the P^0 signal in the undeformed sample with the residual signal P_d^0 in the deformed one ($P^+ = P^0 - P_d^0$). Table II lists the result of such measurements.

Several things can be seen: The ionization of the phosphorus donor increases in the identically deformed samples 1 and 3 with the doping level (and for constant n with the plastic strain ϵ as can be seen from Fig. 13). Within the experimental errors its ionization can neither be influenced by the gas ambient (samples 5 and 6) nor by a predeformation (samples 1,2, or 3,4). However, there is a a tendency that predeformation or deformation in argon gas ambient may increase the phosphorous ionization.

It follows from Table II that the concentration of the defects N_t in sample 3 with energy levels deeper than the phosphorus level is at least 7.3×10^{15} cm^{-3} ($[N_t] \geq [P^+]$) and, therefore, larger than the initial phosphorous concentration of sample 1 (4.4×10^{15} cm^{-3}). But there is still a strong (1.3×10^{15} cm^{-3}) signal of P^0 present in sample 1 even though N_t depends on ϵ (Ref. 6) and should be equal in samples 1 and 3. Thus, the concentration of deformation-induced defects N_t needs to be considerably larger than the initial doping to ionize all P^0 atoms and this indicates a less homogeneous spatial distribution of the deformation induced defects with respect to the chemical dopants.

D. Photo-ESR of samples deformed at 650 °C

Figure 6 shows the increase of the P^0 ESR signal as a function of the light energy as first reported by Erdmann.[10] The spectral dependence of the signal is significantly different from what is observed for the dislocation related defects Si $K1$ and Si $K2$.[7] It should be recognized that in this case the deformation caused an ionization of 8.3×10^{15} P atoms/cm^3, which is at least a factor of 20 larger than the concentration of Si $K1$ and Si $K2$ ($\approx 4\times10^{14}$ cm^{-3}). Thus, their contribution to the ionization of the P donor is negligible and it must be caused by other deformation-induced defects.

Figure 7 shows that the photo-ESR spectrum of the HT signal is rather similar to the one of the phosphorous (Fig. 6): After an increase between 0.45 and 0.65 eV the signals rapidly grow up to 0.75 eV and subsequently increase less steeply up to the band edge and most astonish-

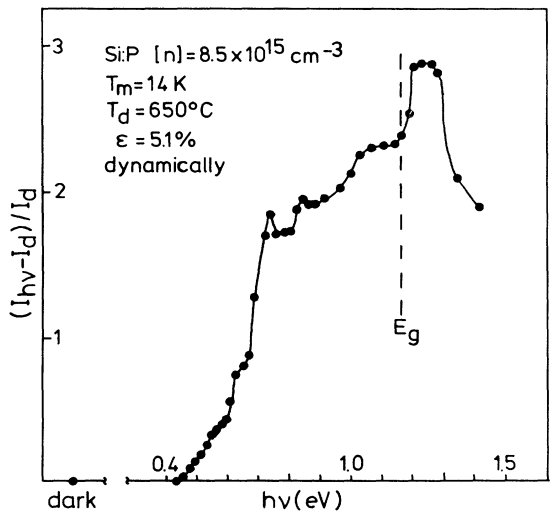

FIG. 6. Photo-ESR spectrum measured on the P^0 resonance. The data are taken from Ref. 10. I_d is the line amplitude of the P^0 signal in darkness while $I_{h\nu}$ is its amplitude measured during illumination of the sample with photons of energy $h\nu$. E_g = band-gap energy.

ingly there is a maximum in the over-band-gap region at 1.24 eV for both signals. However, the photo-ESR spectrum of the P^0 donor is more structured which can be explained by the fact that in Fig. 6 the line amplitude I of the signal can be measured while the investigation of the HT signal requires an integration procedure because it is formed by a variety of different paramagnetic centers which cannot be separated completely.[3]

The kinetics of the photo effect suggests a distinction of the excitations in the over-band-gap region from that within the band gap: The increase of the signals in the over-band-gap region can only be observed during illumination of the sample and it breaks down as soon as the illumination is switched off, while the former leads to persistent signal amplitudes on the time scale of minutes. Erdmann found a logarithmic decay of the P^0 signal when the illumination was removed.[10]

The result suggests that the energy levels of the defects contributing to the HT signal are deeper than 0.45 eV measured from the conduction-band edge and that they are paramagnetic only if lying above the Fermi level. Thus, a simultaneous ESR detection of P^0 resonance and the HT signal in one sample at low detection temperature ($T_d < 30$ K) requires local shifts of the band edges of at least 450 meV in agreement with the results of Sec. III C.

It is instructive that the distinction of photo effects close to the band edge from those deep in the band gap is related to the presence of deep defects *or* dislocations: Figures 8 and 9 show the photo-ESR results of two *n*-type samples one which was compensated by neutron irradiation while the other was plastically deformed and annealed with the aim to remove the deformation induced defects but not the dislocations.[11] The photo-ESR results of the irradiation-induced deep defects in the energy range 0.45–0.8 eV (Fig. 8) are very similar to the behavior of the P^0 and HT signals in this energy range. One of those defects from its ESR spectrum can be identified to be the pentavacancy Si $P1$ which can also be produced by plastic deformation and it contributes to the HT signal.[12] However, there is no further excitation towards the band-gap energy or in the over band-gap region. After illumination the signals decay on the time scale of minutes. Photo-ESR measurements on the P^0 signal could not be performed because of the strong compensation of the sample. In contrast the P^0 signal of the dislocated sample (Fig. 9) shows an excitation only in the near- and over-band-gap region, which proves that his effect is closely related to the presence of dislocations.

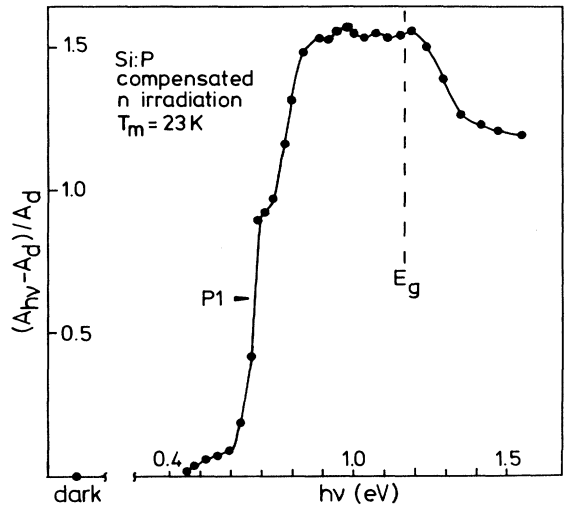

FIG. 8. Photo-ESR spectrum measured on defects introduced by neutron irradiation. Due to the same spin-lattice relaxation of these defects and the HT signal they can be recorded with the same detection parameters as in Fig. 7. $P1$ labels the pentavacancy identified by its ESR spectrum. It can also be produced by plastic deformation (Ref. 12).

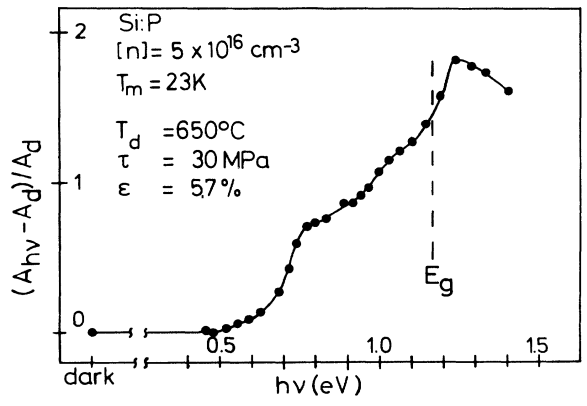

FIG. 7. Photo-ESR spectrum measured on the HT signal of sample *j*. The integrated HT signal $A = \int \chi' dH$ is used because there are contributions of different paramagnetic defects to the signal which cannot be separated. Same subscripts as in Fig. 6.

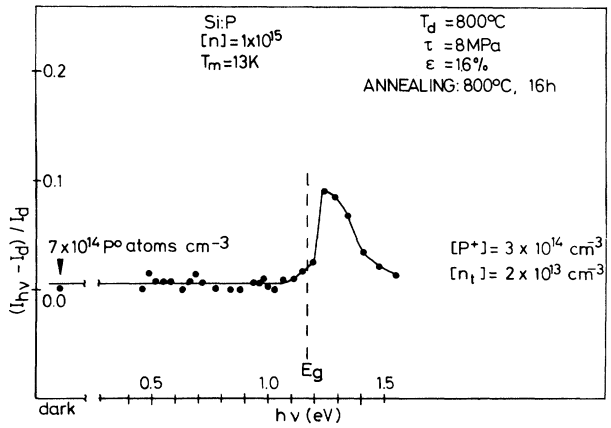

FIG. 9. Photo-ESR spectrum measured on the P^0 resonance of a high-temperature deformed and annealed sample as indicated. From comparison of the signal amplitude in the undeformed sample (initial doping) the number of ionized P^+ atoms can be calculated. The trap density n_t was determined by DLTS measurements (Ref. 13).

Switching off the illumination the signal immediatelly drops to its dark value.

In addition it can be seen from Fig. 9 that after deformation about 3×10^{14} phosphorus atoms per cm^{-3} are ionized and this ionization cannot be explained by the presence of deep-level defects (the number of which was determined by DLTS measurements[13]) because it is much smaller as indicated in Fig. 9.

E. Photo-ESR and ESR spectra of high-stress low-temperature deformed crystals with negligible amounts of deep defects

By use of high-temperature deformation with subsequent annealing followed by high-stress, low-temperature deformation samples with well-defined arrangements of dislocations and negligible amounts of deep defects can be produced as long as the second main deformation is kept small ($\epsilon \ll 1\%$).[13] Detecting the phosphorus photo-ESR spetrum in the undeformed and deformed sample (Fig. 10) reveals an ionization of 3.2×10^{14} P atoms cm^{-3} and a dominant over-band-gap excitation just as in the case of Fig. 9. There is some excitation in the band-gap region due to residual deep defects which is why after illumination the dark value increases as indicated by the arrow in Fig. 10.

The photo-ESR spectrum of the undeformed sample demonstrates that it is not compensated by unknown impurities because the capture of holes is the only process which influences the signal amplitude and it leads to a signal reduction.

As shown in the inset of Fig. 11 there is an additional (anisotropic) ESR signal detectable in such samples and its photo-ESR spectrum is characterized by some excitation within the band gap and a strong decrease of the signal with over-band-gap illumination. Again, switching off the illumination immediately restores a signal amplitude which was reached before by below-band-gap excitations of 0.8–1.1 eV as indicated by the arrow in Fig. 11. From its kinetics it is again attributed to charge coming from residual point defects. The ESR signal itself exhibits uncommon properties: It shows a Dysonian line shape,[14] its signal amplitude depends on the angle of the external magnetic field **H** with respect to the sample orientation, and it grows with the amplitude of the *electric* microwave field E_w as was checked by increasing the sample diameters taking into consideration the distribution of E_w in the TE_{102} cavity used for the experiments. Thus, the increase of the P^0 signal in Fig. 10 is accompanied by a decrease of the ESR signal. Both processes are fast at 15 K.

F. Quantitative comparison of the signals

In order to convert the intensity of the different signals of Figs. 1, 3, and 5 into spin densities we used the following results. In Ref. 8 it has been shown that deformation of sample (*a*) leads to a room-temperature ESR-absorption signal of 3.8×10^{15} spins/cm^3 and in Ref. 6 it was proved that this is the main contribution to the HT-dispersion signal. Thus, one may scale the intensities of the room temperature and the HT signal of sample (*a*) to this value which by comparison gives the corresponding spin densities in all other samples.

However, to convert the abscissa of Fig. 5 from the initial doping to the effective doping (n_e or p_e) it is necessary to know the contributions of the deep and shallow defects to this value. n_e and p_e are estimated in Ref. 13 for a deformation at 650 °C ($\tau=30$ MPa, $\epsilon=2.7\%$) to be: $n-n_e \approx p-p_e \approx N_t=(2-3)\times10^{15}$ cm^{-3} for $n,p>N_t$; for $N_t>>n,p$ the samples are typically highly Ohmic *p* type[15] below room temperature independent of the initial

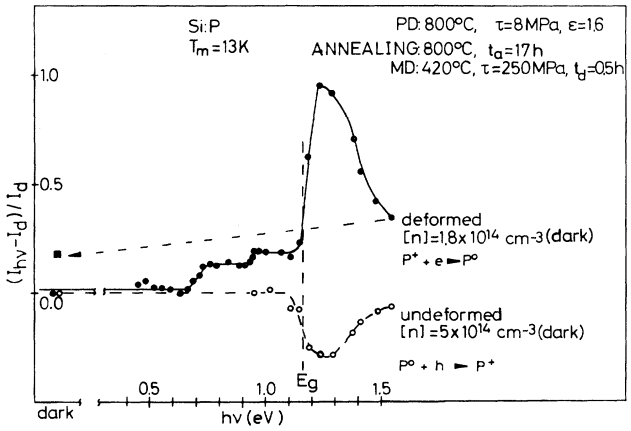

FIG. 10. Photo-ESR spectrum measured on the P^0 resonance in a three-step deformed sample. PD denotes predeformation, MD denotes main deformation. For comparison it is shown that in case of an undeformed sample the capture holes can be recorded which leads to a signal reduction. The arrow indicates the signal amplitude immediately after switching off the illumination. Excitations within the band gap are caused by residual amounts of point defects.

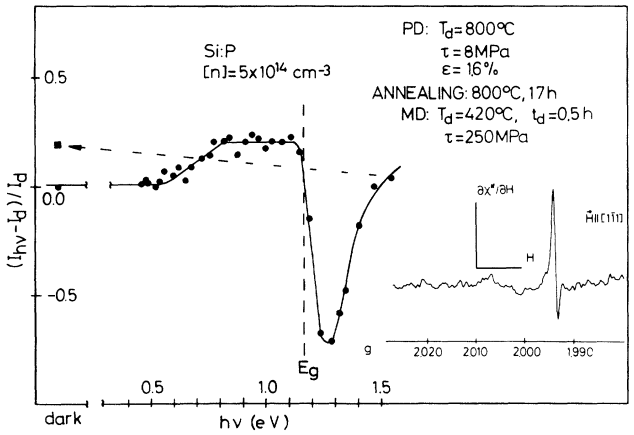

FIG. 11. Photo-ESR spectrum measured at ≈10 K on a ESR signal the absorption spectrum of which is shown in the inset. The arrow indicates the signal amplitude immediately after switching off the illumination. Deformation parameters are indicated.

type of conductivity which demonstrates that the deformation-induced defects are amphoteric and behave acceptorlike in n-type silicon and donorlike in p-type material[13,15] ($N_a \approx N_d \approx N_t$).

This is the way Fig. 12 is constructed. It can be seen that the largest defect concentrations of $(7.5–8.5)\times10^{15}$ cm^{-3} could be measured for the illuminated HT signal in n-type material while the dark concentrations of the signals show a maximum in the p-type region. The 300-K absorption signals and the HT dispersion signals show the same tendencies as expected because the same defects contribute to both signals. In contrast the concentration of Si Y is constant in the weak doping range on a level of $\approx 1.5\times10^{15}$ cm^{-3}. The determined ratio, spins (HT signal) to spins (LT signal) is approximately 3–4,[2,6,16] turns out to be true only for the highly Ohmic material and obviously depends on the doping and on the fact whether the signals are detected in the dark or under illumination. This is a further proof that both kinds of signals are of different origin.

In Fig. 13 the concentration of ionized P atoms is plotted versus the plastic strain for different initial doping levels n. Their number is compared with the spin densities of the 300-K ESR absorbtion signal measured in high Ohmic samples. The shaded area indicates the experimental error. It can be seen that in the low-doped materials ($n \leq 4.4\times10^{15}$ cm^{-3}) the P^+ concentration is smaller than the spin density and it tends to saturate at the initial doping level. However, even in the heavily deformed sample ($\epsilon=5.6\%$ and $n=4.4\times10^{15}$ cm^{-3}) a residual amount of P^0 atoms can be detected ($[P^0]\approx 1\times10^{14}$ cm^{-3}). Ionization of all P atoms is achieved for $\epsilon=3.3\%$ and $n=1\times10^{15}$ cm^{-3}. From this data point it can be estimated that the spin density of the 300-K ESR absorption spectrum needs to be at least four times larger than the initial doping to ionize all P atoms.

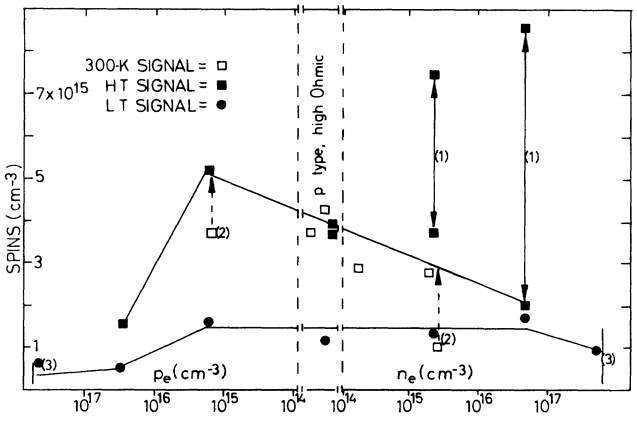

FIG. 12. Spin density of the different signals as a function of the effective doping. For details see text. (1) Signal increase due to illumination with white light; (2) signal amplitude is expected to be corrected into the indicated direction because of the skin effect in conducting samples; (3) experimental error due to superpositions of other signals.

In the case of the high doping ($n=1.1\times10^{16}$ cm^{-3}) the P^+ concentration slightly exceeds the concentration of paramagnetic defects in Fig. 13. From comparison with Fig. 12 it can be seen that the concentration $P^+=7.3\times10^{15}$ cm^{-3} of sample 3 (Table II, Fig. 13) is very close to the concentration of HT centers which can be ionized by illumination (Fig. 12, symbol 1): N (HT, ill.)$-N$(HT, dark)$\approx 6.5\times10^{15}$ cm^{-3} for $n=5\times10^{16}$ cm^{-3} and $\epsilon=2.7\%$). This comparison also holds for the other illuminated sample (Fig. 12, symbol 1): N(HT, ill.)$-N$(HT,dark)$\approx 3.5\times10^{15}$ cm^{-3}, and $[P^+]=3.1\times10^{15}$ cm^{-2}, Fig. 13). Since in addition the photo-ESR results on the neutral P^0 atoms (Fig. 6) and on the HT centers (Fig. 7) show very similar spectral dependences we proved that in the case of strong n doping most of the HT centers ($\approx 75\%$) can be charged by capturing electrons from the shallow donor and, thereby, both the phosphorus atoms and the defects contributing to the HT signal are not paramagnetic anymore. Also, in the case of high doping one would expect that $[P^+] \geq$ [HT centers] because not all acceptorlike defects need to be paramagnetic.

In the case of low doping the usual situation to be detected is the one shown in Fig. 2: There is the ESR signal of P^0 as well as a larger concentration of *paramagnetic* HT centers ($[P^+] <$ [HT centers]) which in the case of higher doping *would* capture electrons and, thereby, lose

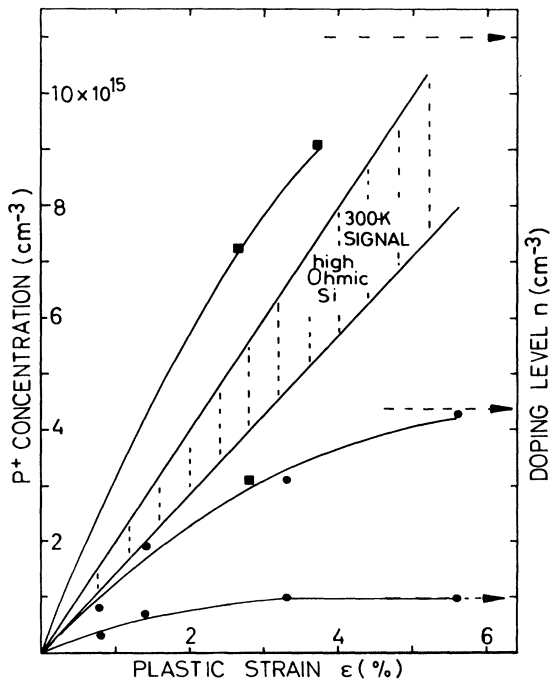

FIG. 13. Concentration of ionized P atoms plotted vs the plastic strain in samples deformed along the [213] axes at 650 °C ($\tau=30$ MPa). On the right-hand side the initial doping level is marked by arrows. The shaded area indicates the spin density of the 300 K ESR absorption signal measured in highly Ohmic material (Refs. 6, 7, and 31). Squares: values of samples 1, 3, and 5 from Table II; circles: values taken from Ref. 30.

their paramagnetism. From Fig. 6 the energy levels of paramagnetic HT centers $E(\mathrm{HT}) \leq E_c - 0.45$ eV can be estimated. Thus, the coexistence of paramagnetic P^0 atoms in addition to such paramagnetic HT centers requires $E_F \geq E(P) = E_c - 0.045$ eV and $E_F \leq E_c - 0.45$ eV, respectively. This is possible if the restrictions are valid *locally,* only, and requires an inhomogeneous distribution of the centers contributing to the HT signal with respect to the presumedly homogeneous distribution of the chemical donor.

IV. DISCUSSION

Typical models of band-gap perturbations in deformed crystals involve band-gap inhomogeneities caused by the trapping of charge on dislocation lines.[17] However, our results suggest that there are different mechanisms leading to similar effects but being of different origin.

The first conclusion from our measurements is that the dominant contribution to the capture of electrons from shallow donors in samples deformed at 650 °C comes from centers which contribute to the HT signal. Thereby, the paramagnetism of both, the donor atoms and the HT signal vanishes. There is a quantitative agreement between the concentration of ionized P atoms and charged HT centers (Sec. III F). The inverse process can be stimulated by photoexcitation the spectral dependence of which is very similar for the HT centers and the P^0 signal (Sec. III D). Spectral differences are attributed to the fact that the P^0 resonance comes from a well-defined defect while the HT signal is a superposition of different paramagnetic centers which were attributed to point defect clusters formed during the deformation procedure.[3] Thus the shallow dopants are compensated by the deformation-induced point defects. As to their position in the band gap the photo-ESR results suggest that they are deeper than $\approx E_c - 0.45$ eV (Figs. 6 and 7). Uncertainties come from the fact that the quartz cryostat used in our experiments absorbs all light with energy $E_{h\nu} \leq 0.4$ eV. This limitation requires use of other experiments which fix their energy positions more accurately.[13] It is also likely that the quartz absorption from our cryostat contributes to the fact that we could not observe electron excitations from the valence band to the defect levels.

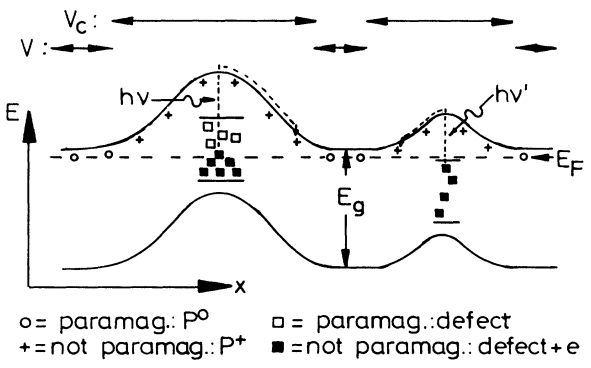

FIG. 14. Schematics of a spatially (x) inhomogeneously compensated crystal. V_c, regions compensated by defects which are paramagnetic only if lying above the Fermi level E_F; V, regions where E_F is close to the level of the shallow donor. Excitation by below-band-gap illumination transfers electrons from the deep defects to the phosphorus atoms as indicated. The width of the defect band on the energy scale is estimated from the photo-ESR results and from Ref. 13.

Difficulties arise from the inhomogeneous distribution of the defects. In the case of doping levels below 10^{16} cm^{-3} and moderate deformations ($\epsilon = 2-3\,\%$) the *local* defect density is large enough to compensate the chemical dopants but there are still regions where the Fermi level is close to the phosphorus level. This situation is schematized in Fig. 14. One may estimate the percentage of the compensated crystal volume V_c with respect to the total volume $V_t = V + V_c$ from Fig. 13 assuming that the percentage of the ionized P atoms with respect to the initial doping is proportional to V_c with respect to V_t. For a deformation of 2.7% the estimation gives $V_c = +90\%$, 70%, and 64% for increasing initial doping n. It is reasonable that V_c decreases with increasing n for a constant trap density because V_c depends on both, the exact spatial distribution of the defects and the screening length which itself depends on the initial doping and the compensation.[18] Nothing is known about the charge states of the defects but from Fig. 12 it must be concluded that the majority of the HT centers must have more than one energy level in the band gap to explain the maximum of the curve.

So far there is no need to discuss special properties of dislocations. They contribute to the picture considering the reason for the inhomogeneous distribution of the defects: It is proposed[11] that they are formed during the motion of dislocations. In the case of defects which are immobile during the deformation procedure they should be distributed in the slip plains of the dislocation. In the case of mobile defects they could form defect clouds around dislocations or they could be accumulated in areas of high local dislocation densities (dislocation walls).

The second point where dislocations need to be considered is again related to the structural informations obtained from ESR: The defects contributing to the LT signal (Si $K1$ and Si Y) are due to structural defects in the core of screw dislocations.[19] But since they are deep and *localized* defects their contribution to the band bending will practically be undistinguishable from those of point defects. Their investigation includes the additional difficulty that their contribution to the balance of charges is rather small: The charge state of Si $K1$ can be changed by doping[9] but its concentration is much smaller than the one of the point defects ($\leq 4 \times 10^{14}$ cm^{-3}). On the other hand the concentration of Si Y is larger but its charge state is hardly affected by doping for reasons which will be discussed in Ref. 13. Thus, they may well contribute to charges on dislocations but the effect can easily be hidden from the contributions of the point defects particularly because they will participate in screening a charged dislocation.

An investigation of undisturbed dislocations is possible by use of deformation and annealing procedures (Fig. 9). The total charge involved in such electrical effects is

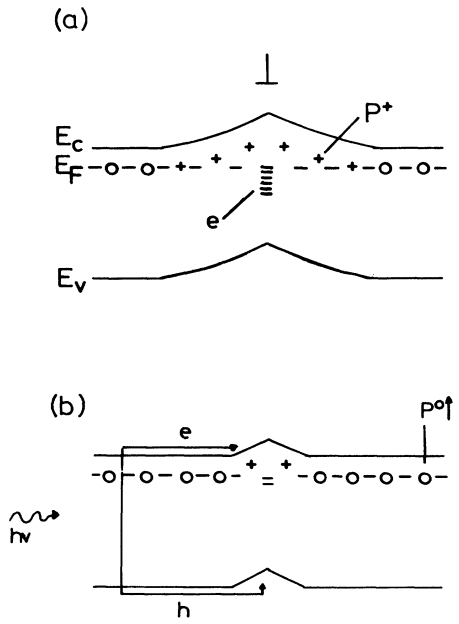

FIG. 15. (*a*) Schematics of a band-gap inhomogeneity caused by electrons trapped in tails of the conduction band at dislocation. (*b*) Generation of electrons and holes by over-band-gap illumination reduces the band bending by hole capture on dislocations and electron capture on the P^+ atoms which leads to the increase of the P^0 resonance.

more than one order of magnitude smaller than what has been discussed for the point defects. The photoexcitations near the band edge (Figs. 9 and 10) can be explained on the basis of Fig. 15 which assumes the existence of dislocation-related states split off from the band edges (perhaps tail states) where electrons can be also trapped (Fig. 15, part (*a*)]. In the case of generation of electron-hole pairs which requires the over-band-gap excitations the holes will be captured to the negatively charged dislocation and the electrons on the ionized donor atoms resulting in an increase of the P^0 resonance [Fig. 15, part (*b*)]. From our experiments it is not directly possible to attribute a certain energy position *within* the band gap to such states.

There are several experiments which give evidence for the existence of such (tail) states: As to the three-step deformation described in Sec. III E it has the additional advantage to produce a well-defined dislocation structure with dislocation lines running parallel to the three [011] directions within a slip plain[20] and the crystals contain negligible amounts of deformation-induced defects. In such crystals a strong microwave conductivity in shallow levels is observed which in the case of photoexcitation shows identical spectral dependences and kinetics as the photo-ESR spectrum of the signal shown in Fig. 11.[21] From its *g* tensor the signal was attributed to electrons on 60° dislocations.[22] Wattenbach[23] recently showed that the particular signal properties arise from the delocalization of electrons along the dislocation line and that the signal is due to electric dipole spin resonances (EDSR).[24] Also, in *p*-type material deformed in a similar way EDSR signals and microwave conductivity in shallow states are observed.[25,26] EDSR signals in deformed crystals were observed in Ref. 27 before and attributed to the presence of *straight* Lomer-Cotrell dislocations which stresses the important role of straight dislocation segments. Also, such split-off or tail states could be observed best by infrared measurements of deformed and annealed samples.[28] Their formation was attributed to dislocation related deformation potentials.

In the neutron-irradiated sample such over-band-gap effects could not be observed (Fig. 8) which supports the point of view that they are restricted to the presence of dislocations. It is satisfactory to recognize that the combination of the photo-ESR spectra of the neutron-irradiated sample (Fig. 8) with the sample containing only dislocations (Fig. 9) gives the basic features of the photo-ESR spectra of deformed samples containing both dislocations and point defects such as those shown in Figs. 6 or 7. Also interesting, neutron irradiation and plastic deformation generate defects in comparable energy ranges of the band gap and by analyzing the structural features of the ESR spectra it was shown that pentavacancies could be produced by both procedures.

Our results are well comparable with those published in Ref. 29 where mostly low-phosphorus-doped samples were used ($\approx 10^{15}$ cm^{-3}). However, the authors never succeeded in ionizing all phosphorous atoms even though the deformation-induced deep defects exceeded our concentrations ($\geq 10^{16}$ cm^{-3}). Only a small fraction of the defects ($\leq 20\%$, filling factor $f \leq 0.2$) could capture electrons. From the presence of both signals the HT centers and the P^0 resonance they concluded that the defects are related to the core of dislocations and that Coulomb repulsion prevents them from being charged. From our results, however, it must be concluded that the local concentration of defects with respect to the chemical donors determines the amount of charge which can be captured from the shallow to the deep defects (Secs. III C and III F). Up to 75% of the deep defects could be charged in our case (Fig. 12). Thus, the spatial distribution of the deformation-induced deep point defects turns out to be even more important than the Coulomb repulsion. Indeed, the authors of Ref. 27 used crystals deformed along their [011] axis which favors multiple slip and by cutting processes the formation of dislocation wall structures. Thus, an even more inhomogeneous distribution of the defects can be expected which makes the ionization of the donor atoms more difficult. Further investigation of the problem requires TEM observations.

Consequently, models which involve a spatial separation of the charge accumulated on a dislocation from the screening ions[17] can probably only be applied to the deformed and annealed samples with negligible amounts of deep defects while in samples deformed below 700 °C the dominant effect consists of a random mixture of positive and negative ions and the application of statistical models as, for example, outlined in Ref. 32 would be adequate.

Moreover, the simple pictures shown in Figs. 14 and 15 do not yet include the formation of states split off from the band edges which could locally narrow the band gap.

As to the possibility that chemical donors (or acceptors) are structurally involved into the formation of the deep defects which could make them electrically inactive[33] we consider this unlikely for two reasons. First, the large concentration of the defects contributing to the HT signal would require that most of the P atoms can be gettered by moving dislocations even at deformation temperatures as low as 420 °C.[3] Secondly, the result of Ref. 29 which showed that parallel with the annealing of the deformation-induced point defects in *n*-type material the ESR signal of isolated phosphorous atoms reappears excludes this possibility explicitly. However, as to the ESR signals which we observed it needs to be clarified whether P or B are structurally involved in the formation of the defects.

V. CONCLUSION

A quantitative analysis of photo-ESR and ESR results of plastically deformed *p*- and *n*-type silicon shows that the charge state of deformation-induced point defects can strongly be influenced by doping. For *n*-type silicon evidence is given that their spatial distribution varies inhomogeneously with respect to the chemical dopants resulting in local distortions of the band edges. Apart from the structural information obtainable from ESR spectroscopy it is hardly possible to distinguish contributions of deep-point defects from those of deep dislocation related defects to the band bending. Controlling the amount of point defects it is possible to separate effects caused by delocalized charges accumulated in shallow dislocation states from those related to the transfer of charge from the dopants to deep localized defects. The last effect is dominant in the case of typical deformations below ≈ 700 °C while the other is observed best in low-doped crystals with negligible amounts of deep defects and it gives rise to the appearance of additional ESR signals. Their observation requires the presence of straight dislocation segments in the crystals.

ACKNOWLEDGMENTS

R. Meurer and M. Hühne participated in ESR measurements of ionized P atoms. The Deutsche Forschungsgemeinschaft supported the project financially. Professor E. R. Weber supplied the neutron irradiated sample.

[1]H. Alexander, in *Point and Extended Defects in Semiconductors,* edited by G. Benedek, A. Cavallini, and W. Schröter (Plenum, New York, 1989), p. 51.

[2]Yu. A. Osip'yan Sov. Sci. Rev. A **4**, 219 (1982); Phys. Rev. **4**, 219 (1982).

[3]C. Kisielowski-Kemmerich and H. Alexander, Fiz. Tver. Tela (Leningrad) **31**, 254 (1989) [Sov. Phys.—Solid State **31** 864 (1989)].

[4]L. Bartelsen, Ph.D. thesis, Universität Köln, 1976; Phys. Status Solidi B **81**, 471 (1977).

[5]U. Voermanns, C. Kisielowski-Kemmerich and H. Alexander, in *Science and Technology of Defect Control in Semiconductors,* edited by K. Sumino (Elsevier, Amsterdam, 1990), p. 1357.

[6]C. Kisielowski-Kememrich, G. Weber, and H. Alexander, J. Electronic Mater. **14a**, 387 (1985).

[7]R. Erdmann and H. Alexander, Phys. Status Solidi A **55**, 251 (1979).

[8]C. Kisielowski-Kemmerich, J. Czaschke, and H. Alexander, Mater Sci. Forum **10-12**, 745 (1986).

[9]M. N. Zolotukhin, Fiz. Tver. Tela (Leningrad) **28**, 3306 (1986) [Sov. Phys.—Solid State **28**, 1862 (1986)].

[10]R. Erdmann, Ph.D. thesis, Universität Kön, 1979.

[11]C. Kisielowski-Kemmerich and H. Alexander, in *Defects in Crystals,* edited by M. Mizera (World Scientific, Singapore, 1988), p. 270.

[12]M. Brohl, C. Kisielowski-Kemmerich, and H. Alexander, Appl. Phys. Lett. **50**, 1733 (1987).

[13]C. Kisielowski and E. R. Weber, preceding paper, Phys. Rev. B **44**, 1600 (1991).

[14]F. J. Dyson, Phys. Rev. **98**, (1955).

[15]V. A. Grazhulis, V. V. Kveder, and V. Yu. Mukhina, Phys. Status Solidi A **43**, 407 (1977).

[16]V. A. Grazhulis and Yu. A. Osip'yan Zh. Eksp. Teor. Fiz. **58**, 1259 (1970) [Sov. Phys.—JETP **31**, 677 (1970)].

[17]R. Labusch and W. Schröter, in *Dislocations in Solids,* edited by F. R. N. Nabarro (North-Holland, Amsterdam, 1980)), p. 127.

[18]F. Stern, Phys. Rev. B **9**, 4597 (1974).

[19]C. Kisielowski-Kemmerich, in *Structure and Properties of Dislocation in Semiconductors,* edited by S. G. Roberts, D. B. Holt, and P. R.Wilshaw, IOP Conf. Proc. No. 104 (Institute of Physics and Physical Society, London, 1989), p. 187.

[20]K. Wessel and H. Alexander, Philos. Mag. **35**, 1573 (1977).

[21]M. Brohl, M. Dressel, H. W. Helberg, and H. Alexander, Philos. Mag. B **61**, 97 (1990).

[22]J. Krüger, Diploma thesis, Universität Köln 1988.

[23]M. Wattenbach (unpublished).

[24]E. I. Rashba, Usp. Fiz. Nauk **84**, 557 (1964) [Sov. Phys. Usp. **7**, 823 (1965).

[25]M. Wattenbach, C. Kisielowski-Kemmerich, H. Alexander, V. V. Kveder, T. R. Mchedlidze, and Yu. A. Osip'yan, Phys. Status Solidi B **158**, K49 (1990).

[26]M. Brohl, Ph.D. thesis, Köln Universität, 1990; M. Brohl and H. Alexander, in *Structure and Properties of Dislocations in Semiconductors,* Ref. 19, p. 163.

[27]V. V. Kveder, T. R. Mchedlidze, Yu. A. Osip'yan, and A. I. Shalynin, Solid State Phenom. **6&7**, 1989, 301.

[28]A. V. Bazhenov and L. L. Krasil'nikova, Fiz. Tver. Tela (Leningrad) **28**, 235 (1986) [Sov. Phys.—Solid State **28**, 128 (1986)].

[29]V. A. Gradzhulis and Yu. A. Osip'yan, Zh. Eksp. Teor. Fiz. **60**, 1150 (1971) [Sov. Phys.—JETP **33**, 623 (1971)].

[30]J. Michel, Diploma thesis, Universität Köln, 1983.
[31]C. Kisielowski-Kemmerich, Ph.D. thesis, Universität Köln, 1985.
[32]B. I. Shklovskii and A. L. Efros, in *Electronic Properties of Doped Semiconductors,* edited by M. Cardona, Solid State Sciences Vol. 45 (Springer, Berlin, 1984).
[33]M. I. Heggie, R. Jones, G. M. S. Lister, and A. Umerski, in *Structure and Properties of Dislocations in Semiconductors,* Ref. 19, p. 163.